Module 8: Optical Detectors

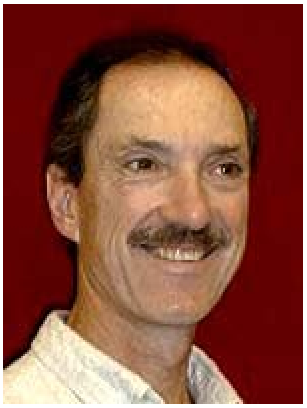

Dr. Raymond K. Kotsuk

Professor of Electrical and Computer Engineering, University of Arizona

Dr. Raymond K. Kotsuk is a Professor of Electrical and Computer Engineering in the University of Arizona. His areas of research include holographic techniques, systems, and materials, ion exchange waveguide devices - interfacing to polymer and PBG layers, fiber optic systems including OCDMA, error-correction codes, all-optical network issues, medical imaging sensors including OCT and holographic filtering of coherent image data.

Email: kostuk@ece.arizona.edu

Introduction

Optical detectors are used to convert the optical information transmitted over the fiber into an electrical signal. It is the interface between the optical and electronic domain. Most detectors used in fiber communications are semiconductor devices so we will be examining different semiconductor structures and geometries that have proven to be useful. We will also investigate the absorption properties of semiconductors and the resultant responsivity to optical radiation.

8.1 Optical Detectors

Optical fiber communication systems are comprised of three essential components:

- The source, with its associated modulators to transform electrical communications signals into the optical signals;
- The fiber, to transmit the light and sometimes to amplify it; and
- The optical detector, to receive the optical signal and transform it back to an electrical signal that is recorded and stored or used to operate an output device such as a speaker.

The transmitted optical signal intensity and the plausible communications distance are dependent on the optical signal intensity of the source, the loss per distance of the fiber and the detection sensitivity of the detector. As such, the detection process is a vital aspect of the optical communications system’s performance.

The authors would like to acknowledge support from the National Science Foundation through CIAN NSF ERC under grant #EEC-0812072.

In these applications the detectors we will consider convert incident light to a coded electrical current. Since they produce electrical power, which is proportional to the current squared, these are often called *square law devices*.

Although there are many forms of optical detectors we will primarily discuss pn junction, pin (a pn junction diode with an intrinsic layer), APD (avalanche photo diode), and MSM (metal-semiconductor-metal) photodiodes since these are most widely used in optical communications systems.

Detector Parameters:

When characterizing a detector, three of the most important parameters are:

1. Responsivity, *R*
2. Modulation bandwidth (BW)
3. Noise characteristics

The detector responsivity is related to the absorption properties of the semiconductor used to fabricate the detector.

Responsivity is based on the *efficiency*, η, of converting photons to electrons.

η = *(Number of electrons generated)/(Number of incident photons)*

$$\eta = \frac{I_{ph} / q_e}{P_o / h\nu} \qquad \textbf{(Equation 8.1)}$$

I_{ph} is the current generated by incident photons, q_e is the fundamental unit of charge; P_o is the incident optical power illuminating the detector surface; and $h\nu$ is the photon energy. As indicated the efficiency is the ratio of the rate of electron generation per rate of incident photons.

In calculating the number of electrons generated, one also needs to consider the probability that a photon will be absorbed after propagating a distance x into the material and produce an electron-hole pair. This is given by:

$$\left[1 - e^{-\alpha x}\right], \qquad \textbf{(Equation 8.2)}$$

where α is the absorption per unit length in the detector material. This result is determined from basic absorption properties of materials. Consider a small cell with area *A* and populated with *N* targets with an absorption cross-section σ.

The authors would like to acknowledge support from the National Science Foundation through CIAN NSF ERC under grant #EEC-0812072.

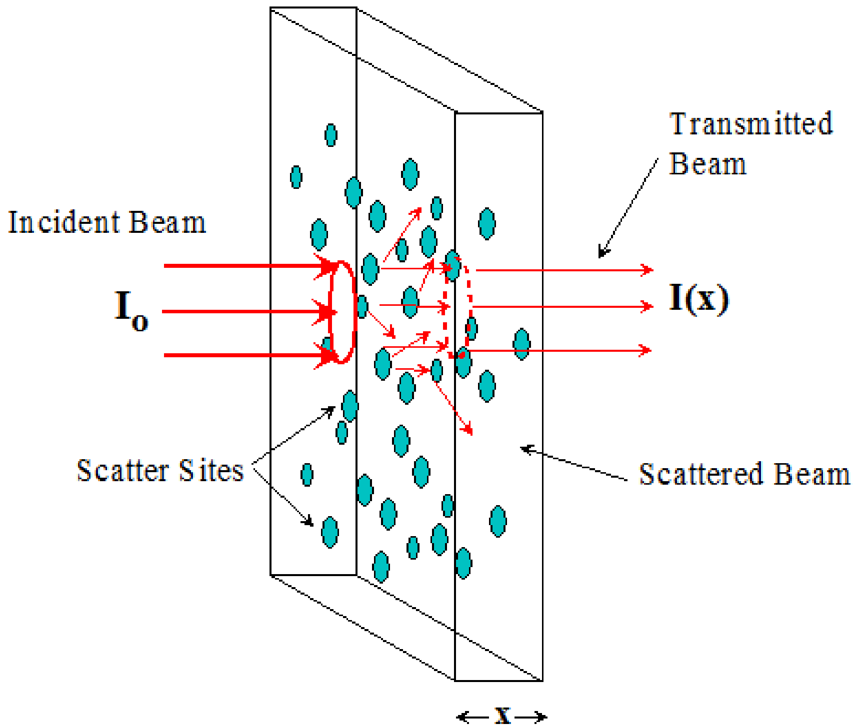

Figure 8.1

As photons pass through this cell they hit the targets and do not pass through the cell. The total target area in the cell is $\sigma ANdx$ and the fraction of photons passing through the cell is σNdx. The reduction in power per unit area of the optical beam is $dI = -\sigma NIdx$. Integrating this relation results in

$$\ln I = -\sigma NIx + B\,. \quad \textit{(Equation 8.3)}$$

For a cell of thickness x, the change in power per unit area between the entrance and exit surface is:

$$\ln I_o - \ln I(x) = \sigma xN \quad \textit{(Equation 8.4)}$$

The corresponding transmittance becomes:

$$T = \frac{I(x)}{I_o} = e^{-\sigma Nx} = e^{-\alpha x} \quad \textit{(Equation 8.5)}$$

And the absorption is:

$$\left[1 - e^{-\alpha x}\right]. \quad \textit{(Equation 8.6)}$$

The authors would like to acknowledge support from the National Science Foundation through CIAN NSF ERC under grant #EEC-0812072.

The units used for the absorption coefficient is per unit length (i.e. cm^{-1}). The absorption coefficient is measured by illuminating a sample of material with known thickness with light at different wavelengths of known power. The experimental arrangement is similar to the figure above illustrating absorption.

The external quantum efficiency of the detector is

R_r is the *intensity reflection* coefficient at the detector surface, and d is the effective thickness of the detector material. This efficiency relation assumes that each absorbed photon results in the formation of an electron-hole pair that results in current generation at the output terminals of the detector. If this is not the case an additional η_{int} factor must be included in the total efficiency calculation.

$$\eta = \eta_{\text{int}}\left(1 - R_r\right) \cdot \left(1 - e^{-\alpha d}\right) \qquad \textit{(Equation 8.7)}$$

Absorption coefficients for several detector materials are shown in the figure below. The ordinate on the left is the absorption coefficient per centimeter and on the right the depth in micrometers. The abscissa is the wavelength of light illuminating the semiconductor in micrometers. Si – silicon; GaAs – gallium arsenide; and InGaAs – indium gallium arsenide.

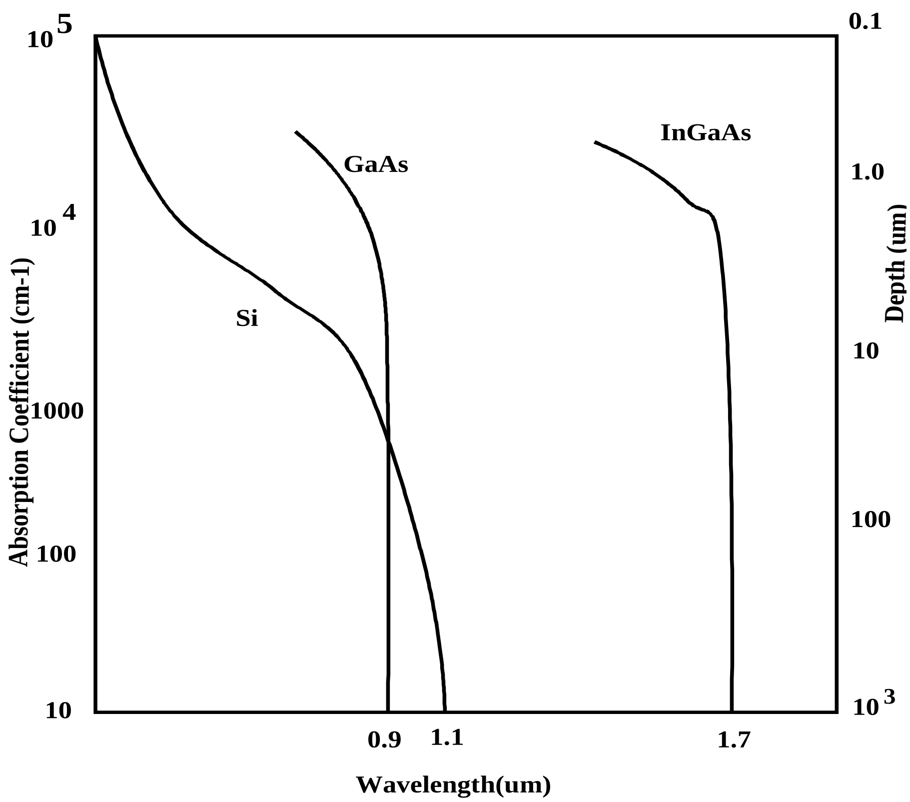

Figure 8.2

The authors would like to acknowledge support from the National Science Foundation through CIAN NSF ERC under grant #EEC-0812072.

The cut-off wavelengths for different materials in the above Figure represent the wavelength corresponding to the band gap energy: $E_g = h\nu = hc/\lambda$. The material does not detect energies below the band gap energy (i.e. wavelengths larger than the cut-off wavelength).

The absorption coefficient α is given in nepers per meter.

The Responsivity is related to the conversion efficiency by the relation:

$$R = \frac{I_{ph}}{P_o} = \frac{\eta q}{h\nu}\left(\frac{A}{W}\right) \qquad \textit{(Equation 8.8)}$$

This is a very useful parameter because it indicates the electrical current produced in response to the optical power illuminating the detector surface. The optical power is computed from the irradiance E(power/area) and the area of the detector A_{det} using the relation:

$$P_o = E \cdot A_{det} \qquad \textit{(Equation 8.9)}$$

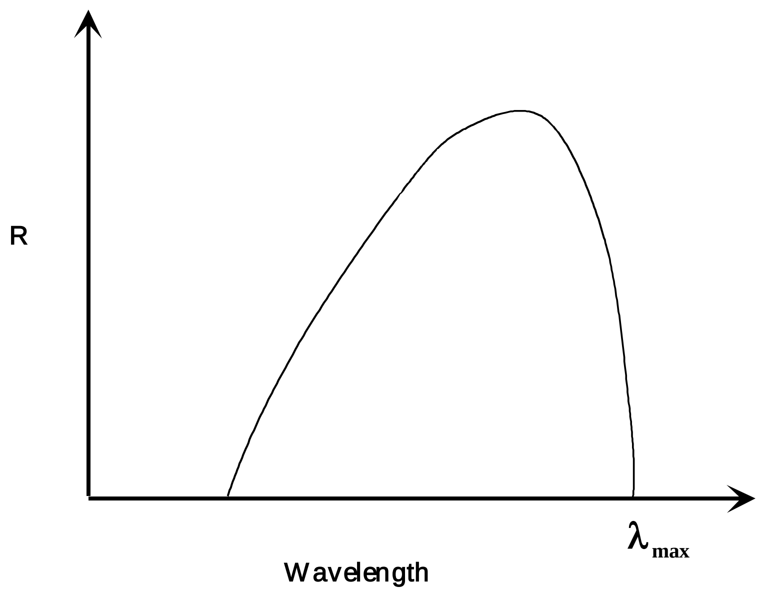

***Figure 8.3** : The above figure is a general plot of the responsivity vs. optical wavelength for a material with a bandgap, i.e. a semiconductor. The maximum wavelength corresponds to the minimum energy needed to move an electron across the bandgap.*

The *maximum wavelength* for which there is significant response can be determined from the band gap energy using the relation:

The authors would like to acknowledge support from the National Science Foundation through CIAN NSF ERC under grant #EEC-0812072.

$$\lambda_{\max}(\mu m) = \frac{1.24}{E_g(eV)} \qquad \text{(Equation 8.10)}$$

The wavelength is in units of micrometers and the band gap energy is in units of electron volts. The factor $1.24 = hc/q$ is in units of micrometers.

Notice that materials with smaller band gap energies have longer cut-off wavelengths. They are more sensitive to thermal effects where energies that can be imparted to electrons are on the order of kT where k is the Boltzmann constant and T is the temperature in degrees Kelvin.

8.2 p-n Junctions

The majority of detectors used in optical communications systems are based on p-n and p-i-n type junctions in semiconductors. The p- refers to an acceptor (Na) type doped semiconductor, n- a donor (Nd) doped semiconductor, and i- indicates an intrinsic or un-doped semiconductor. In this module the properties of these junctions will be examined as relates to the process of high-speed signal detection.

Depletion Layer

In a p-n junction, a space charge region (also called a depletion layer) forms at the interface of the two material types. This region is shown as the area with width `W' in the figure below. It has several properties:

- This region is depleted of most free carriers as they are drawn into the n-type or into the p-type material.
- This region has a natural electric field that pushes any electrons created in the region toward the n-type material and any hole toward the p-type material.
- If a photon generates an electron-hole pair in this region the charges move rapidly at the drift velocity induced by the electric field.
- If a charge pair is formed outside of this region they move to the terminals by diffusion at a much slower rate.
- The junction is typically reversed biased to increase the width of the space charge region. This can be accomplished by applying a voltage with positive polarity connected to the `n' side of the diode and negative polarity to the `p' side, illustrated in Figure 8.4.

The authors would like to acknowledge support from the National Science Foundation through CIAN NSF ERC under grant #EEC-0812072.

Also shown in Figure 8.4 is the optical power as a function of penetration depth into the p-n diode. As indicated a large fraction of the incident illumination reaches regions outside the space charge width. This results in many electron-hole pairs being generated in parts of the p-n junction where diffusion dominates as a charge transport mechanism.

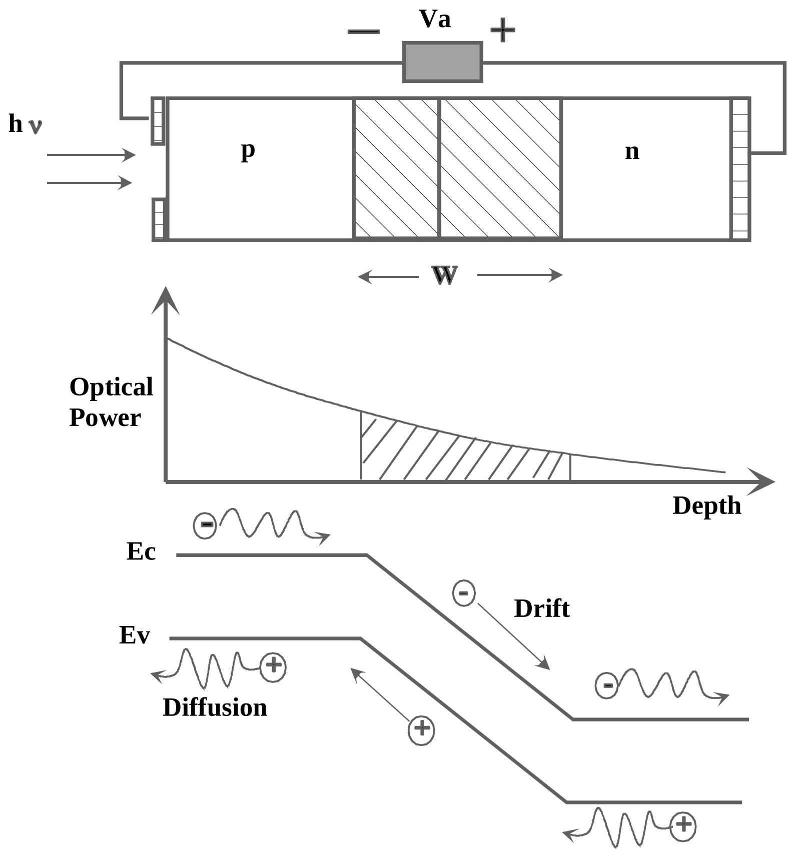

Figure 8.4 ***The lower illustration in the above figure shows the conduction and valence bands across the p-n junction and the movement of charges within the space-charge region and in the quasi-neutral n- and p-type areas.***

Junction Equilibrium

Under equilibrium conditions the flow of electrons from the n to p side and holes from the p to n side of the junction due to diffusion must be balanced. Charge carriers move either by diffusion forces or through drift currents set up by the electric field formed at the junction. If an abrupt boundary is assumed between the n and p type materials the charge balance can be expressed using the one dimensional Gauss's Law:

$$qN_a x_p = qN_d x_n = \varepsilon_s \varepsilon_o E \qquad \textit{(Equation 8.11)}$$

The authors would like to acknowledge support from the National Science Foundation through CIAN NSF ERC under grant #EEC-0812072.

where x_p and x_n are respectively the extent of the depletion regions on the p and n side of the junction, ε_s is the relative dielectric constant of the semiconductor, and E is the electrostatic field established across the junction. This relation also establishes the `depletion approximation', which implies that the total (+) ionized charge on the n side equals the (-) ionized charge on the p side.
Using Poisson's equation across the junction provides an expression for the voltage:

$$-\frac{d^2V}{dx^2}=\frac{dE}{dx}=\frac{q}{\varepsilon_s\varepsilon_o}\left[p(x)-n(x)+N_d(x)+N_a(x)\right]. \quad \textit{(Equation 8.12)}$$

It follows that

$$\begin{aligned}-\frac{d^2V}{dx^2}&\approx\frac{q}{\varepsilon_s\varepsilon_o}N_d, 0<x\le x_n\\ -\frac{d^2V}{dx^2}&\approx\frac{q}{\varepsilon_s\varepsilon_o}N_a, -x_p<x\le 0\end{aligned}. \quad \textit{(Equation 8.13)}$$

Integrating to obtain the electric field yields:

$$\begin{aligned}E(x)&=\frac{qN_d}{\varepsilon_s\varepsilon_o}(x-x_n)\\ &=\frac{qN_a}{\varepsilon_s\varepsilon_o}(x+x_p)\end{aligned} \quad \textit{(Equation 8.14)}$$

on the two sides of the junction. If the expression for the E field is integrated the potential across the junction is found:

$$V(x)=E_{\max}\left(x-\frac{x^2}{2W}\right), \quad \textit{(Equation 8.15)}$$

with E_{max} being the maximum field at the junction. The maximum field occurs at x = 0 and substituting the values from the field expression provides working functions for the potentials in the space charge region as a function of position:

$$\begin{aligned}V(x)&=-\frac{qN_d}{\varepsilon_s\varepsilon_o}(x-x_n)^2\\ &=-\frac{qN_a}{\varepsilon_s\varepsilon_o}(x+x_p)^2\end{aligned}, \quad \textit{(Equation 8.16)}$$

and the built-in potential across the junction from the n to the p side is:

$$V_{bi}=\frac{q}{2\varepsilon_s\varepsilon_o}\left[N_a x_p^2+N_d x_n^2\right]. \quad \textit{(Equation 8.17)}$$

The authors would like to acknowledge support from the National Science Foundation through CIAN NSF ERC under grant #EEC-0812072.

As stated earlier in equilibrium the drift and diffusion currents must cancel. The electron and hole current densities in the depletion region can be expressed as:

$$J_n = q\left(n\mu_n E + D_n \frac{dn}{dx} \right) = 0$$
$$J_p = q\left(p\mu_p E - D_p \frac{dp}{dx} \right) = 0 ,$$ **(Equation 8.18)**

where $\mu_{n,p}$ is the carrier mobility and $D_{n,p}$ is the diffusion coefficient satisfying the Einstein relation;

$$D_{n,p} = \frac{\mu_{n,p} k_B T}{q} .$$ **(Equation 8.19)**

The diffusion coefficient, minority carrier diffusion length, and minority carrier lifetime are related through $L_{n,p} = \sqrt{D_{n,p}\tau_{n,p}}$.

Assuming full ionization of the dopants, the above relations can be used to find the built-in potential in terms of the fabrication parameters:

$$V_{bi} = \frac{k_B T}{q} \ln\left(\frac{N_a N_d}{n_i^2} \right).$$ **(Equation 8.20)**

The depletion layer width can also be found using the expression for the maximum field:

$$\varepsilon_s \varepsilon_o E_{\max} = qN_d x_n = qN_a x_p .$$ **(Equation 8.21)**

Since

$$\left|V_{bi}\right| = \frac{E_{\max}}{2}\left(x_n + x_p \right),$$ **(Equation 8.22)**

the total width of the depletion region $W = x_n + x_p$ is equal to:

$$W = \left[\frac{2\varepsilon_s \varepsilon_o}{q} \left(\frac{1}{N_a} + \frac{1}{N_d} \right) \left|V_{bi}\right| \right]^{1/2} .$$ **(Equation 8.23)**

The depletion region can be considered to be a capacitor with a capacitance given by:

$$C = \frac{\varepsilon_s \varepsilon_o A}{W},$$ **(Equation 8.24)**

where A is the area of the junction. Substituting the relation for W results in:

The authors would like to acknowledge support from the National Science Foundation through CIAN NSF ERC under grant #EEC-0812072.

$$C = \frac{\varepsilon_s \varepsilon_o A}{\left[\frac{2\varepsilon_s \varepsilon_o}{q} \left(V_{bi} - V_a \right) \frac{N_a + N_d}{N_a N_d} \right]^{1/2}}, \qquad \textbf{(Equation 8.25)}$$

where V_a is an additional applied voltage across the diode. The capacitance will affect the frequency response of the detector and it can be seen from the last relation that an applied voltage can be used to change the capacitance.

A p-n junction is formed by growing an n(p) type semiconductor followed by the growth of a p(n) type material. Silicon has 4 electrons in its outer shell. Phosphorous has 5 electrons in its outer shell and will act as a donor impurity in a semiconductor of silicon atoms. Boron has 3 electrons in its outer shell and will act as an acceptor atom in silicon. In both cases, one assumes that the impurity atom concentration is small so that the impurity atom sits in the structure at a substitutional impurity for silicon. Since silicon, with 4 electrons, has a tetrahedral stricture, when phosphorus is a substitutional impurity, it also sits in a tetrahedral structure which only requires 4 electrons. The fifth electron in Phosphorus is “donated” to the semiconductor. Boron has only 3 electrons. When it sits in a tetrahedral structure, it lacks a fourth electron and this forms a hole which can “accept” a free electron. At some concentration, the impurities begin to form alloys and the dopant atoms no longer adopt the structure of the host and form their own structure. This determines the maximum doping level possible.

The PIN Photodiode

In order to increase the *space-charge region* and minimize *diffusion current* components an *intrinsic layer* (undoped layer) is introduced to the diode structure at the interface between the n-type and p-type materials. The intrinsic material is not doped with donor or acceptor atoms so has relatively few mobile carriers. This effectively stretches the space charge region and increases the volume of material where carriers are separated at drift velocities. It also reduces the volume of material where carriers move by diffusion while keeping the absorption length for photons the same (same total material thickness).

The authors would like to acknowledge support from the National Science Foundation through CIAN NSF ERC under grant #EEC-0812072.

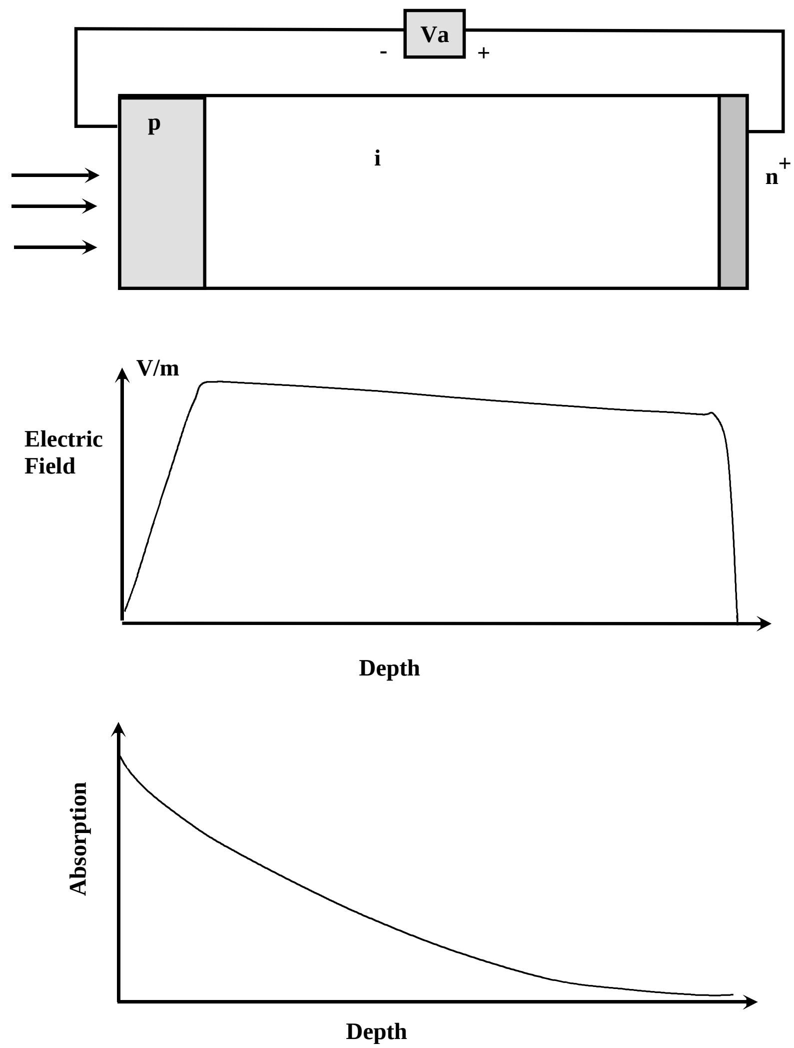

Figure 8.5

8.3 Other Detectors used in Communication Systems

The Avalanche Photodiode

The gain or electrical signal amplitude (current) generated by a flux of photons is proportional to the number of photons absorbed and the number of carriers generated at a rate of one electron-hole pair per photon.

The authors would like to acknowledge support from the National Science Foundation through CIAN NSF ERC under grant #EEC-0812072.

One approach to *increase the gain* of a detector is to use ***internal amplification*** effects. This can be accomplished by changing the structure of the diode and applying an external voltage to increase the ***reverse bias potential***.

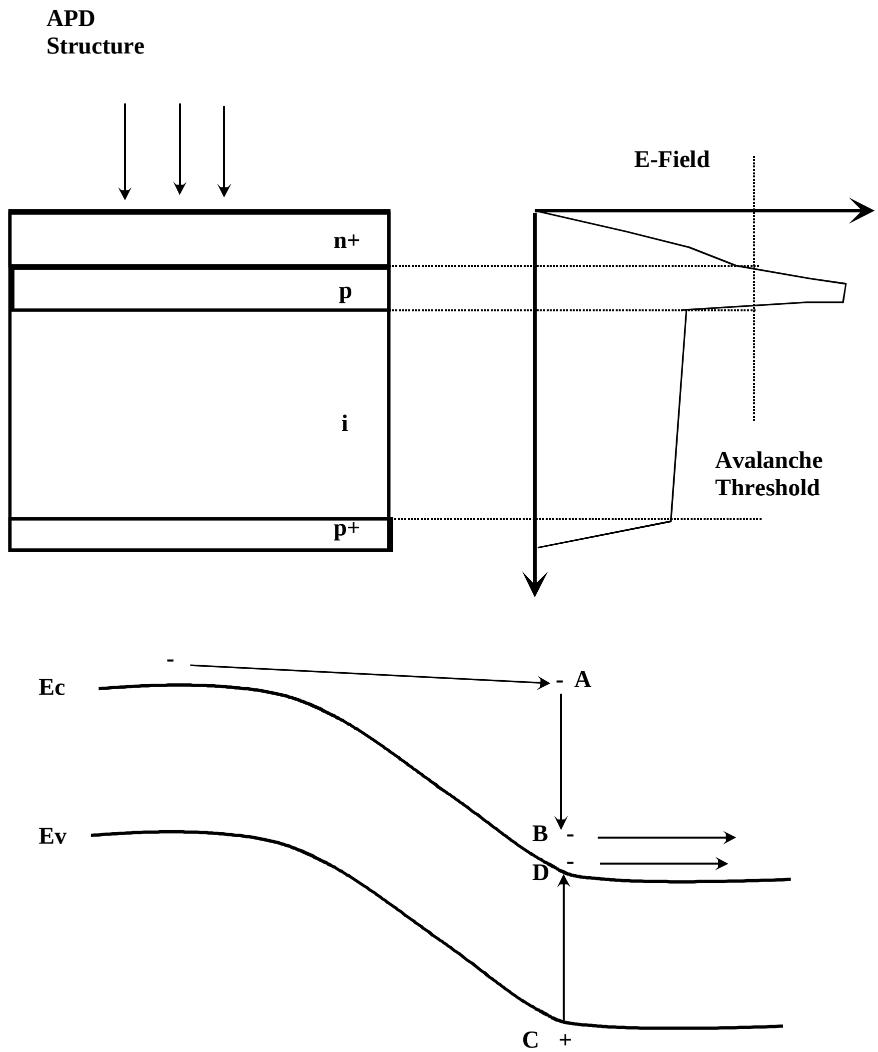

Figure 8.6 ***Diagram of an APD semiconductor structure (upper left), the electric field within the structure (upper right), and the energy bands across the junction (lower).***

Most of the applied reversed bias potential is dropped across the n^+-p region resulting in a high internal field (~3×10^5V/cm). This accelerates charge carriers to high velocities (*high kinetic energy A*) and through collisions or ***impact ionization*** (C) these form new carriers. These carriers then accelerate and form additional carriers (B, D).

The net effect of the avalanche process is a multiplication of the current at the output. This is usually specified in terms of a ***multiplication factor M***.

The authors would like to acknowledge support from the National Science Foundation through CIAN NSF ERC under grant #EEC-0812072.

$$M = \frac{I_M}{I},$$ *(Equation 8.26)*

where I_M is the current with multiplication and I is the current without multiplication.

An optimum bias voltage range is reached after the initial rise in multiplication factor. Increasing the voltage too much leads to a ***run away avalanche effect*** (***Zener Breakdown***).

The multiplication factor will also affect the noise characteristics of this detector. This will be discussed later in the noise section of this chapter.

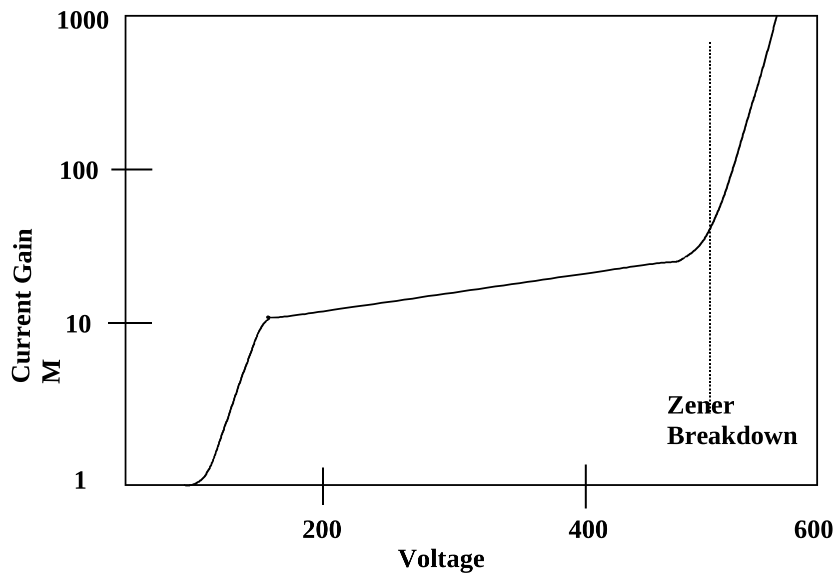

Figure 8.7 *The current gain as a function of the reverse bias potential applied across an APD.*

The ***responsivity*** of the APD is

$$R_{APD} = \frac{\eta q \lambda}{hc} M = R_o M$$ *(Equation 8.27)*

where R_o is the *responsivity* of the photodiode without gain.

The Metal-Semiconductor-Metal Photodetector

Another type of detector that is important for fiber communication systems is the metal-semiconductor-metal (***MSM) device***.

This detector is formed with ***two Schottky contacts*** (semiconductor-metal) on an undoped semiconductor layer.

The authors would like to acknowledge support from the National Science Foundation through CIAN NSF ERC under grant #EEC-0812072.

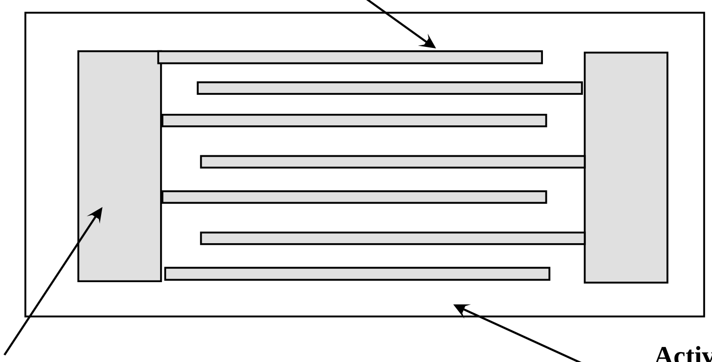

Figure 8.8 ***Top view of an MSM detector showing the metal contacts on the surface.***

This photodetector design has several characteristics:

- The ***finger spacing*** between contacts is about *~1* μm and the ***width*** of the electrodes is approximately the same distance.
- In the *Schottky photodiode* structure $\phi - \chi$ is the potential barrier between the metal and the semiconductor
- ϕ is the ***work function*** - the minimum energy required to free an electron from the metal (or semiconductor) is the difference in energy between the Fermi level and the vacuum level.
- χ the ***electron affinity*** (the energy difference between the bottom of the conduction band (E_c) and the vacuum level) is the energy needed to free an electron from the semiconductor.

The authors would like to acknowledge support from the National Science Foundation through CIAN NSF ERC under grant #EEC-0812072.

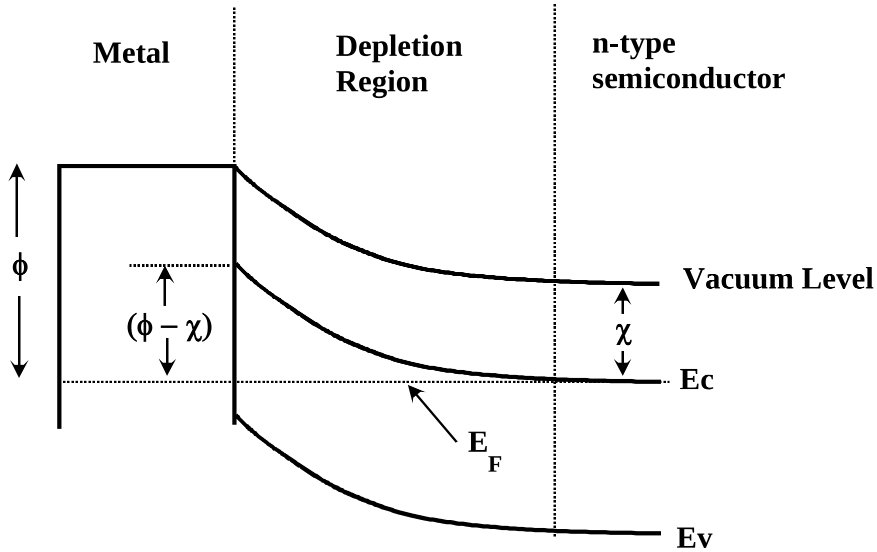

***Figure 8.9** Energy bands at a metal-semiconductor (Schottky) junction. A depletion region forms at the interface much like in a p-n junction.*

The *metal contacts* reduce the *responsivity* since part of the incident light is blocked. But, improvements to responsivity have been made by reducing the thickness of the electrodes and illuminating the detector from the bottom.

Values on the order of 0.4-0.7 A/W at 1.55 μm have been achieved. However, bottom illuminated detectors have lower bandwidths.

Bandwidths of 20-50 GHz have been achieved and it may be possible to go to 100 GHz with refinements to MSM devices.

8.4 Noise Sources and Characterization

Noise refers to a variation in the signal level about some average value. Optical communications detectors are generally operated in reverse bias mode. This reduces the dark current and shot noise resulting from charge generation within the depletion region. Therefore thermal noise tends to be dominant but can be reduced with proper circuit design. In this section the noise that occurs with an incoming modulate optical signal will be evaluated.

The authors would like to acknowledge support from the National Science Foundation through CIAN NSF ERC under grant #EEC-0812072.

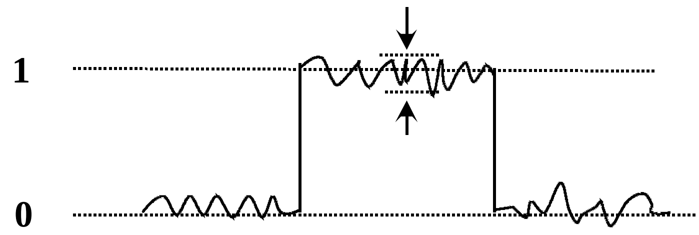

Figure 8.10 *Diagram illustrating a `0' and a `1' signal that would be received by a detector and the fluctuation or noise that may be encountered with these signals.*

Thermal Noise

At finite temperatures electrons move randomly in a conductor, this occurs in load resistors in optical receivers.

The detector is usually connected to a pre-amplifier that has a resistance of R_{in} which is in parallel with R_L. The equivalent resistance of the detector/receiver can be expressed as:

$$\frac{1}{R_{eq}} = \frac{1}{R_{sh}} + \frac{1}{R_L} + \frac{1}{R_{in}}. \qquad \textit{(Equation 8.28)}$$

The mean square thermal noise current is:

$$\overline{i_{th}^2} = \frac{4k_B T}{R_{eq}}. \qquad \textit{(Equation 8.29)}$$

where T is the absolute temperature in Kelvins and B_e is the effective bandwidth.

Shot Noise

Shot noise is a result of the fact that electric current consists of a stream of electrons that are generated at random times. Consider an incident optical signal:

$$P(\omega) = P_o\left(1 + me^{j\omega t}\right). \qquad \textit{(Equation 8.30)}$$

For simplicity let the modulation index m = 1. The rms optical power is $P_o/\sqrt{2}$ and the resulting rms current is

$$i_o = \frac{q\eta P_o}{\sqrt{2}h\nu}. \qquad \textit{(Equation 8.31)}$$

Generally there will also be a small component of background illumination resulting in a current (I_B) and thermally generated current formed in the depletion region (I_D). The resulting shot noise from these current components is:

The authors would like to acknowledge support from the National Science Foundation through CIAN NSF ERC under grant #EEC-0812072.

$$\overline{i_{sh}^2} = 2q\left(i_o + I_D + I_B\right)BW \ , \qquad \textbf{(Equation 8.32)}$$

where BW is the frequency bandwidth of the receiver.

Signal-to-Noise Ratio (SNR)

The electrical SNR of a detector represents the ratio of the electrical signal power relative to the electrical noise power

$$SNR = \frac{I_p^2}{\left\langle i_N^2 \right\rangle} \qquad \textbf{(Equation 8.33)}$$

Note that the load resistance term cancels from the ratio.
The electrical power corresponding to the optical signal current is $i_o^2 R_{eq}$ and the electrical noise power $\overline{i_N^2} = \left[\overline{i_{sh}^2} + \overline{i_{th}^2}\right] R_{eq}$. The corresponding electrical signal-to-noise ratio:

$$SNR_{pwr} = \frac{\frac{1}{2}\left(\frac{q\eta P_o}{h\nu}\right)}{2q\left(i_o + I_B + I_D\right)BW + \frac{4k_B T}{R_{eq}}BW} . \qquad \textbf{(Equation 8.34)}$$

The detector sensitivity is a measure of performance and can be expressed as the minimum input optical power required to achieve a certain SNR. This can be expressed as a noise equivalent power or NEP. The NEP is computed with a BW = 1Hz and a SNR = 1. Rearranging the previous relation:

$$\frac{q\eta P_o}{\sqrt{2}h\nu} = \sqrt{\overline{i_N^2}} = \left[2q\left(i_o + I_B + I_D\right) + \frac{4k_B T}{R_{eq}}\right]^{1/2} \sqrt{BW} \ , \qquad \textbf{(Equation 8.35)}$$

therefore

$$NEP = \frac{h\nu}{q\eta}\left[2q\left(i_o + I_B + I_D\right) + \frac{4k_B T}{R_{eq}}\right]^{1/2} (W/\sqrt{Hz}) \quad . \qquad \textbf{(Equation 8.36)}$$

From the express for NEP it can be seen that improved sensitivity R_{eq} and η should be as large as possible and I_B and I_D as small as possible. The current i_o is a desirable quantity and remains significant if the detector is shot noise limited.

Relative Intensity Noise (RIN)

The authors would like to acknowledge support from the National Science Foundation through CIAN NSF ERC under grant #EEC-0812072.

This noise source originates with laser transmitters but manifests itself in fluctuations at the detector/receiver.

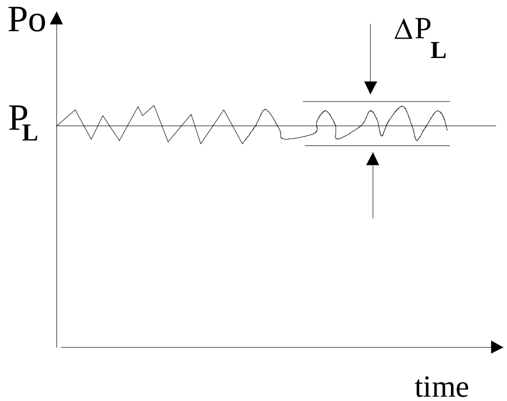

Figure 8.11 ***Figure illustrating the output of an optical source as a function of time and the fluctuation in the output resulting in a fluctuation in a detector.***

The RIN factor expresses the ratio of the fluctuation in electrical output power relative to the average incident electrical power level. Since the optical power is proportional to the electrical current $\left(i = \Re P_o\right)$ the RIN factor can be expressed as the square of the ratio of the fluctuation in received optical power relative to the average received optical power.

$$RIN \cdot B = \frac{\left\langle \left(\Delta P_L\right)^2 \right\rangle}{\overline{P}_L^2} \qquad \textit{(Equation 8.37)}$$

Using this expression we can incorporate it as another noise term along with shot and thermal noise factors for computing signal-to noise ratios.
The expression can be re-written as:

$$\left\langle \left(\Delta i_{src}\right)^2 \right\rangle = \left\langle \left[R\Delta \overline{P}_L\right]^2 \right\rangle = RIN \cdot B\left(R\overline{P}_L\right)^2 \qquad \textit{(Equation 8.38)}$$

$$RIN = 10\log\left[\left(\frac{\Delta P_L}{\overline{P}_L}\right)^2 \Big/ B\right]\left(dB/Hz\right)$$

$$\left(\frac{\Delta P_L}{\overline{P}_L}\right)^2 = 10^{\frac{RIN}{10}} B \qquad \textit{(Equation 8.39)}$$

As an example with a RIN factor ~150 dB/Hz and B = 10^9Hz:

The authors would like to acknowledge support from the National Science Foundation through CIAN NSF ERC under grant #EEC-0812072.

$$\left(\frac{\Delta P_L}{\bar{P}_L}\right)^2 = \left(10^{-15}/Hz\right)\cdot B$$

$$\left(\frac{\Delta P_L}{\bar{P}_L}\right)^2 = \left(10^{-15}\right)\cdot 10^9 = 10^{-6} \qquad \textbf{(Equation 8.40)}$$

$$\therefore \Delta P_L = 10^{-3}\bar{P}_L$$

Noise in APD Detectors

As discussed previously APD detectors provide additional *internal gain*.
This improves responsivity but also affects the noise.

$$\left\langle i_s^2 \right\rangle = 2qM^2 F_A (RP_{in} + I_d) B_e \qquad \textbf{(Equation 8.41)}$$

where F_A is the *excess noise factor* which represents the additional random effects that occur due to the avalanche amplification process (in the worst case F_A ~2; in the best case it is linear with M).

The *thermal noise factor* is not generally affected by M. Therefore the SNR for the APD is:

$$SNR = \frac{(MRP_{in})^2}{2qM^2 F_A (RP_{in} + I_d) B_e + 4(kT/R_L) B_e}. \qquad \textbf{(Equation 8.42)}$$

When *limited by thermal noise* there is an *M^2 improvement* to the SNR for the APD. However when *limited by shot noise* the SNR of the APD is a factor of $1/F_A$ less than the pin photodiode.

Example: Consider a PIN photodiode used in a high impedance receiver with:

R_L = 10 kΩ; C_d = 1 pF; $\Re$ = 0.35 A/W; T = 300°K; and I_{dark} = 1nA
The optical power incident on the detector is P_{in} =1 μW. The corresponding 3dB bandwidth of the receiver is:

$$B_{3dB} = \frac{1}{2\pi R_L C_d} \qquad \textbf{(Equation 8.43)}$$

The resulting electrical SNR is:

The authors would like to acknowledge support from the National Science Foundation through CIAN NSF ERC under grant #EEC-0812072.

$$SNR = \frac{\Re^2 P_{in}^2}{2q\left(\Re P_{in} + I_{dark}\right) B_{3dB} + \frac{4kT}{R_L} B_{3dB}}$$
$$= 1.243\times 10^{10}\left(100.9dB\right)$$ ***(Equation 8.44)***

If the receiver is switched to a transimpedance amplifier:

$$B_{3dB} = \frac{1}{2\pi \frac{R_F}{A-1} C_d} = \frac{A-1}{2\pi R_F C_d}$$ ***(Equation 8.45)***

$$\left\langle i_T^2 \right\rangle = \frac{4kT}{R_F} B_{3dB}$$
$$\left\langle i_{sh}^2 \right\rangle = 2q\Re P_{in} B_{3dB}$$ ***(Equation 8.46)***

Therefore the effective bandwidth of the receiver increases along with the noise factors. This will cause the SNR to decrease.

The authors would like to acknowledge support from the National Science Foundation through CIAN NSF ERC under grant #EEC-0812072.